Supplemental Material for "Formation and reorganization timescales of aeolian landscapes."

Andrew Gunn[1,*]

[1]*School of Earth, Atmosphere & Environment, Monash University, Australia, 3068*

[*]*Corresponding Author: a.gunn@monash.edu*

METHODS

Topographic analysis

We employ the ALOS Global Digital Surface Model to study topography (Tadono et al., 2014). This data is at 1-arcsecond horizontal resolution and 1-m vertical resolution. The full topography field was split into tiles centered on the wind data grid points, which is at 0.1-degree horizontal resolution, so each topographic tile is 360 grid-points long in each dimension. We focus only on the 1,047 tiles in the landscape where bedrock is exposed between the dunes in order to estimate the dune volume. For each of these tiles, we identify the dune volume and area coverage, and for a given wind angle, the average length flux occurs over, the average slope the wind sees, and the average length of dunes (Fig. S1).

To calculate these quantities, we need to mask out the exposed bedrock. We note that this 'bedrock' has been identified as the Eocene Dammam formation overlain in places by Sabkha deposits (Elberg et al., 1963). We do this by first taking the absolute local slope at all grid points on the tile and applying a median filter disk with diameter of 10 arcseconds to it. We define all places on the landscape as bedrock where the values of this field are below a threshold, except the places where the absolute elevation there is one standard deviation of all the tile's topography above the median absolute elevation of the below-threshold-slope topography. This exception needs to be included as some dunes have quite flat surface and would be considered bedrock otherwise. We then mask out all the bedrock to calculate the properties of the dunes (Fig. S1).

The area of dune coverage A_b is simply the summed area of grid points in the tile not considered bedrock. The area fraction $\hat{A}$ is the dune coverage area over the area of the tile A, $\hat{A} = A_b/A$. The dune volume V_b is calculated by looking at cross-sections of the masked topography with constant latitude and integrating the area between the topographic profile of the dune segments and the minimum elevation in the segment. These areas are then integrated across latitude to find volume. The equivalent thickness η is V_b/A (Wasson & Hyde, 1983; Fig. S2), and the average dune height H_b is $\eta/\hat{A}$.

For the wind direction dependent quantities, we first produce equally spaced cross-sections of the topography at that angle with increasing distance defined in the wind direction. The length of dune surface in that direction $\overrightarrow{L_b}$ is defined as the average proportion of these cross-sections including dune topography multiplied by the tile length L. The average wind-facing slope for the tile $\overrightarrow{S_d}$ is defined as the slope from the base of the dune to its peak along the cross-section, weighted by the slope lengths. The average dune length $\overrightarrow{L_d}$ is defined as the average proportion of the cross-section any given dune covers multiplied by the tile length. The dune width is defined as the length in the direction where it is maximized, i.e., $max\{\overrightarrow{L_d}\}$. This process is conducted for 10-degree bins of wind directions.

Sediment flux calculation

We first employ the ECMWF ERA5-Land climate reanalysis from 1981 to 2020 (inclusive; Muñoz Sabater, 2019) to compute the saturated sediment flux from the wind field. ERA5-Land data is currently provided at 0.1-degree horizontal resolution and 1-hour time resolution. We take the 10-m altitude wind vector field $\overrightarrow{u_{10}}$ and calculate the surface friction velocity using the Law of the Wall, $\overrightarrow{u_*} = \overrightarrow{u_{10}}\,\kappa/ln\ (10/z_0)$, where Von Karman's constant is $\kappa = 0.4$ and the roughness length is $z_0 = 10^{-3}$ m. This surface friction velocity field is then used to calculate sediment flux in excess of a threshold friction velocity for sand transport. The threshold is defined as,

$$u_{*,cr} = \alpha\sqrt{gd\,(\rho_s - \rho_f)/\rho_f},$$

After Bagnold (1941), where the dimensionless constant of proportionality is $\alpha = 0.082$, gravity is $g = 9.8$ m/s^2, sediment diameter is $d = 0.3$ mm, sediment density is $\rho_s = 2650$ kg/m^3, and fluid density is $\rho_f = 1.2$ kg/m^3. This gives $u_{*,cr} = 0.21$ m/s. We use these representative constants in lieu of more precise values for the Rub' al Khali. Saturated sediment flux is then defined in the direction of above-threshold winds as,

$$\overrightarrow{q_s} = \gamma\,\rho_f u_{*,cr}\left(\overrightarrow{u_*} - u_{*,cr}\right)^2/g,$$

After Martin & Kok (2017), where the dimensionless constant of proportionality is $\gamma = 5$.

This saturated sediment flux is then adapted using the topographic quantities described above to find the true sediment flux $\vec{q}$. The average true sediment flux across the dune is half the saturated sediment flux at the brink $\overrightarrow{q_{s,br}}$ because flux increases from zero at the dune foot to the brink flux at the brink, then decreases to zero at the toe. This neglects the slip-face, but in our study site most dunes do not have well-defined slip faces. The saturated sediment flux at the brink is higher than the saturated sediment flux because the wind speeds up in proportion to the slope of the dune the wind sees $\overrightarrow{S_d}$. We define,

$$\overrightarrow{q_{s,b}} = \overrightarrow{q_s}\,(1 + \beta\overrightarrow{S_d}),$$

After Courrech du Pont et al. (2014), where the dimensionless value $\beta = 9.44$. We have chosen this value for β such that the average value of $\beta\overrightarrow{S_d} = 1$ for the study site, in accordance with numerous observations and theoretical results for the speed-up of winds hills and dunes (Courrech du Pont et al., 2014; Pugh, 1997; Jackson & Hunt, 1975). The true sediment flux is therefore $\overrightarrow{q_{s,br}}/2$ scaled by the proportion of dune surface seen from that direction,

$$\vec{q} = \overrightarrow{q_{s,br}}\,\overrightarrow{L_b}/2\,L,$$

Such that sand availability is taken into account. This approach assumes that topography is quasi-static over the duration of the computed fluxes; a reasonable assumption since the average distance dunes migrate over 40 years is ~0.02% of the horizontal resolution of the wind data.

Sediment flux analysis

We use the true sediment flux field $\vec{q}(x, y, t)$ found using the method outlined above to compute the rate of elevation change $\partial\eta/\partial t$ and metrics for the true flux like the net flux and the flux directionality (i.e., "RDP/DP"). The rate of elevation change is defined using the Exner equation (Bagnold, 1941; Exner, 1925):

$$\partial\eta/\partial t = -(\partial\vec{q}/\partial x + \partial\vec{q}/\partial y)/\phi\,\rho_s,$$

Where the packing fraction is $\phi = 0.6$. In practice this is produced on an offset grid from the $\vec{q}(x, y)$ field because it is defined between the flux vectors, then it is interpolated back onto the same grid as $\vec{q}(x, y)$. The net flux $\overrightarrow{q_{net}}$ is defined as the sum of the true flux divided by the duration of observation T, $\overrightarrow{q_{net}} = \sum_t \vec{q}/T$. The flux directionality $\hat{q}$ is the ratio of the length of the net flux vector over the length of all flux vectors,

$$\hat{q} = |\textstyle\sum_t \vec{q}|/\sum_t|\vec{q}|.$$

Timescale scaling analysis

The formation timescale T_η is defined as $\eta/(\partial\eta/\partial t)$, and the reorganization timescale T_a is defined as $\overrightarrow{L_d}/c$ where $\overrightarrow{L_d}$ is in the direction of net true flux. The deposition rate is,

$$\partial\eta/\partial t = -(\partial\vec{q}/\partial x + \partial\vec{q}/\partial y)/\phi\,\rho_s,$$

And the migration speed is,

$$c = |\vec{q}|/(H_b\phi\rho_s).$$

The variables in these definitions are defined in the sections above. Note that in general, some dunes may elongate from a source at a rate c instead of laterally translating, but in this study the dunes have non-local sources. We can infer the relative scale of these timescales by taking their ratio, the Mobility number Mo (Jerolmack & Mohrig, 2007), and reducing it. By substituting variables and reducing we can write,

$$Mo = T_\eta / T_a \approx \eta q \Delta L / (L_d H_b \Delta q),$$

Where ΔL is the discretised distance over which the flux change Δq is measured. Now first we note that $H_b = \eta / \hat{A}$, and we define $\hat{L} = L_d / \Delta L$ so that,

$$Mo \approx \hat{A}\, q / (\hat{L} \Delta q).$$

$\hat{A}$ and $\hat{L}$ are less than unity by definition and are approximately equal, and since gradients in q (i.e., Δq across ΔL) aren't larger than its magnitude (strictly positive), we can say that $Mo \gtrsim 1$.

Stratigraphic analysis

We use dune geometry and sediment flux to infer the set thickness and cross-bedding width preserved in dune stratigraphy (Rubin & Hunter, 1982; Brookfield, 1977). The set incline angle θ_δ is angle made by the deposition rate over the migration speed (Brookfield, 1977),

$$tan\theta_\delta = \partial\eta / \partial t / c,$$

And the set thickness δ is the height made by this angle across the dune length (Rubin & Hunter, 1982; Brookfield, 1977),

$$\delta = L_d\, \partial\eta / \partial t / c.$$

The cross-bedding width ε is the product of the migration speed and the time a bed is made. We take this timescale to be the most powerful timescale of transport, the annual cycle, so $\varepsilon = cT_a$. These values lose meaning where the flux directionality is low and are most applicable in unidirectional depositional regime (Rubin & Hunter, 1982). When taking the product of the set thickness and the cross-bedding width, the migration speed c cancels.

We note that the stratigraphic implications of the timescales T_a and T_c depends on the subtle definition of T_c. The climate persistence timescale T_c is not the time that one paleoclimate existed for, it is the duration of time that the climate which existed when stratigraphy was laid down persisted for beforehand. The reason T_c is defined this way is that for any moment in time, including the present day, it is not clear *a priori* how long the climate will persist for in the future.

Study site characterization

We focus on the region in the Rub' al Khali where there is bedrock exposure so that we can measure the dune thickness η. We found this area using Landsat imagery on Google Earth and drew a perimeter around it that was used to mask the wind and topography data. To the northwest, the perimeter delineates the boundary between dunes with and without interdune exposure. To the southeast, the perimeter delineates the edge of the dune field. Landsat imagery inspection shows that all dunes in the study location are unvegetated and have completely erodible surfaces (i.e., full sand availability aside from interdune exposure). We manually identified the typical morphology of the largest dunes within

each of the 1,047 0.1-degree wide tiles centered on the gridded wind data points within this perimeter (Fig. S2). This typical morphology was categorized using standard nomenclature.

DATA AVAILABILITY

The ERA5-Land reanalysis data used in this study are available in the Climate Data Store database https://cds.climate.copernicus.eu/. The ALOS Global Digital Surface Model data used in this study are available in the OpenTopography database https://opentopography.org.

CODE AVAILABILITY

Code to reproduce this paper can be found at https://github.com/geomorphlab/fluxdiv.

SUPPLEMENTAL FIGURES

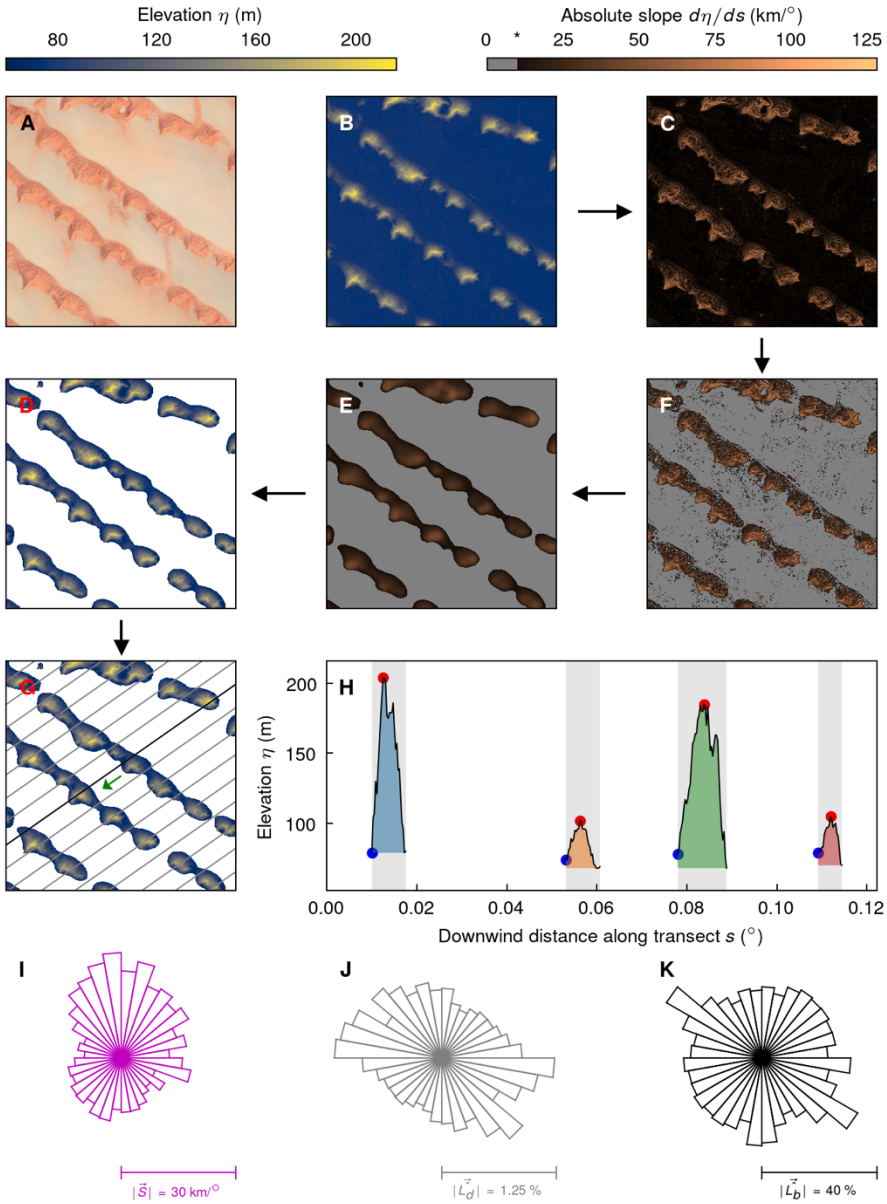

Figure S1: Topography analysis. (A) Satellite imagery of example tile. (B) The elevation map of the example tile from ALOS Global Digital Surface Model; this is centered on an ERA5-Land grid point and has the same width and height as the grid spacing. (C) The maximum absolute slope of the surface from (B). (F) The same as (C) but all values less than a threshold (marked with an asterisk in the color bar) are shaded grey. (E) The output of (F) with at 10-arcsecond median filter disk applied to find areas consistently flat; the non-grey area is considered the area fraction of the dunes. (F) The original topography in (B) with the grey area of (E) masked out; this is considered the dune topography. (G) Transects for directional properties across (D) in in grey with one example transect in black. The green

arrow marks the direction of the transects. (H) The elevation profile along the example black transect in (G), the transect x-axis increases in the direction of the transect. The black lines indicate the dune topography. The shaded area beneath the dunes is bounded by their respective heights and minimum elevations; this is how dune volume is calculated. The grey shaded areas behind the dunes represent their length coverage of the transect. The blue dots indicate the base of the wind-facing slope, whereas the red dots indicate the maximum height of the wind-facing slope. (I) The distribution of average (weighted by the slope lengths) wind-facing slope for this tile across all angles. (J) The distribution of the proportion of transects covered by dunes (average fractional coverage of any single grey shaded area in (H) for all transects, across all angles. (K) The same as (J) but the sum of the grey shaded areas. Scales for the distributions (I-K) are given below each and are defined in the direction a wind encounters them from. Color bar for (B,D,G) in top left; for (C,E,F) in top right. Imagery by Maxar via Google Earth.

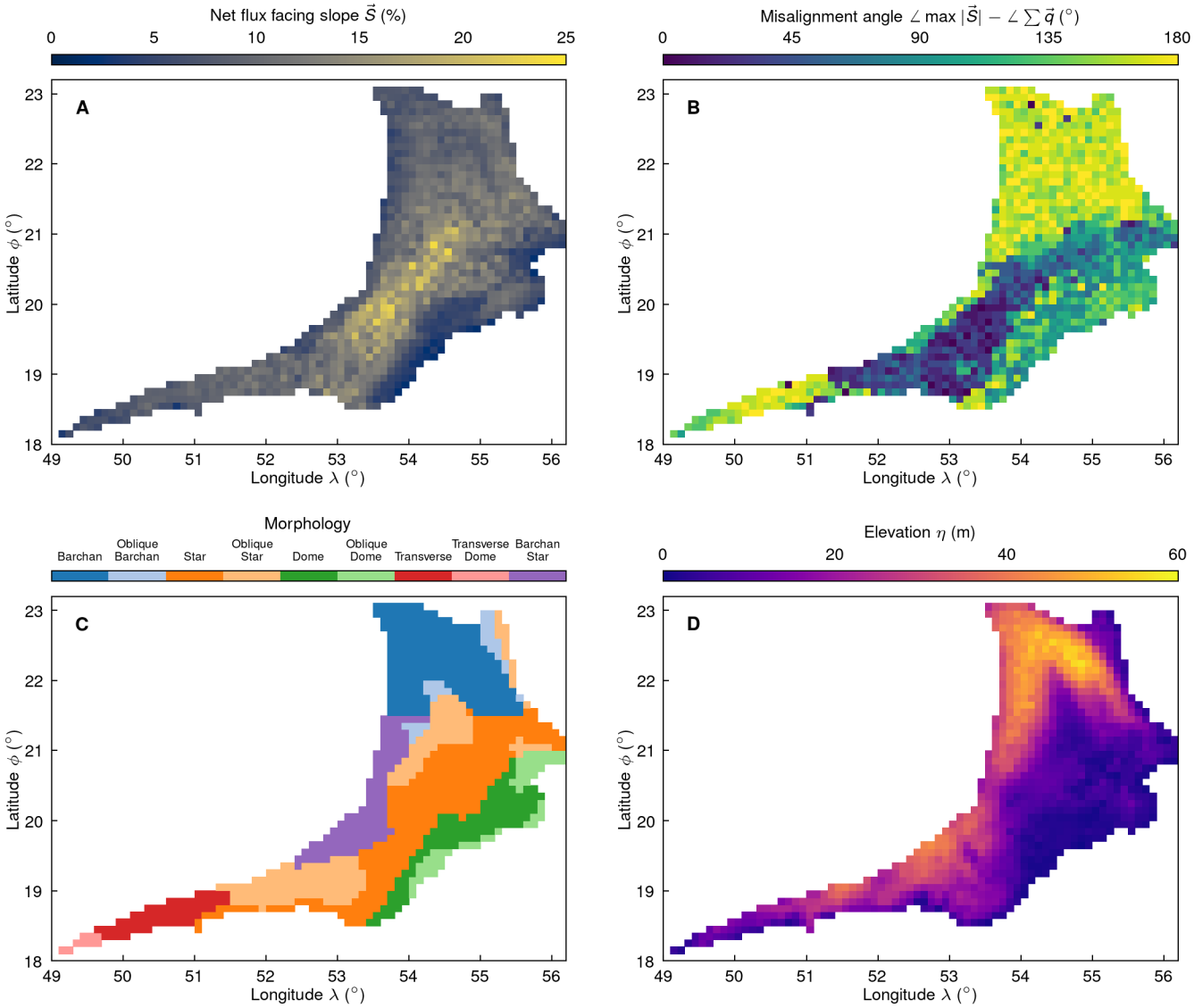

Figure S2: Maps of study area properties. (A) The slope of the dunes facing the net true flux direction. (B) The smallest angle between the steepest slope of the dunes and the net true flux direction. (C) The manually classified morphology. (D) The average elevation of the dunes, i.e., “equivalent thickness”.

REFERENCES CITED

Bagnold, R. A. (1941). *The physics of blown sand and desert dunes*. Courier Corporation.

Brookfield, M. E. (1977). The origin of bounding surfaces in ancient aeolian sandstones. *Sedimentology*, *24*(3), 303-332.

Courrech du Pont, S., Narteau, C., & Gao, X. (2014). Two modes for dune orientation. *Geology*, *42*(9), 743-746.

Elberg Jr, E. L., Gierhart, R. D., & Ramirez, L. F. (1963). *Geologic map of the eastern Rub Al Khali quadrangle, Kingdom of Saudi Arabia* (No. 215-A). US Geological Survey.

Exner, F. M. (1925). Über die wechselwirkung zwischen wasser und geschiebe in flüssen. *Akad. Wiss. Wien Math. Naturwiss. Klasse,* 134(2a), 165-204.

Jackson, P. S., & Hunt, J. C. R. (1975). Turbulent wind flow over a low hill. *Quarterly Journal of the Royal Meteorological Society*, *101*(430), 929-955.

Jerolmack, D. J., & Mohrig. D. (2007). Conditions for branching in depositional rivers. *Geology 35.5*: 463-466.

Martin, R. L., & Kok, J. F. (2017). Wind-invariant saltation heights imply linear scaling of aeolian saltation flux with shear stress. *Science advances*, *3*(6), e1602569.

Muñoz Sabater, J. (2019). ERA5-Land hourly data from 1981 to present. *Copernicus Climate Change Service (C3S) Climate Data Store (CDS)*, *10*.

Pugh, J. M. (1997). *The quaternary desert sediments of the Al Liwa area, Abu Dhabi*. University of Aberdeen (United Kingdom).

Rubin, D. M., & Hunter, R. E. (1982). Bedform climbing in theory and nature. *Sedimentology*, *29*(1), 121-138.

Tadono, T., et al. (2014). Precise global DEM generation by ALOS PRISM. *ISPRS Annals of the Photogrammetry, Remote Sensing and Spatial Information Sciences*, *2*(4), 71.